University of Dundee

OPTICA

Observation of a triangular-lattice pattern in nonlinear wave mixing with optical vortices

B. Pinheiro da Silva,[1,2,*] G. H. dos Santos,[3] A. G. de Oliveira,[3]
N. Rubiano da Silva,[3] W. T. Buono,[4] R. M. Gomes,[5] W. C. Soares,[6] A. J. Jesus-Silva,[7]
E. J. S. Fonseca,[7] P. H. Souto Ribeiro,[3] and A. Z. Khoury[1]

[1]*Instituto de Física, Universidade Federal Fluminense, 24210-346 Niterói, RJ, Brazil*
[2]*School of Science and Engineering, University of Dundee, Dundee, DD1 4HN, Scotland, UK*
[3]*Departamento de Física, Universidade Federal de Santa Catarina, CEP 88040-900, Florianóplis, SC, Brazil*
[4]*School of Physics, University of the Witwatersrand, Private Bag 3, Johannesburg 2050, South Africa*
[5]*Instituto de Física, Universidade Federal de Goiás, CEP 74690-900, Goiânia, GO, Brazil*
[6]*Núcleo de Ciências Exatas—NCEx, Universidade Federal de Alagoas, CEP 57309-005, Arapiraca, AL, Brazil*
[7]*Instituto de Física, Universidade Federal de Alagoas, CEP 57072-970, Maceió, AL, Brazil*
*Corresponding author: braianps@gmail.com

Preparation, control, and measurement of optical vortices are increasingly important, as they play essential roles in both fundamental science and optical technology applications. Spatial light modulation is the main approach behind the control strategies, although there are limitations concerning the controllable wavelength. It is therefore crucial to develop approaches that expand the spectral range of light modulation. Here, we demonstrate the modulation of light by light in nonlinear optical interactions to demonstrate the identification of the topological charge of optical vortices. A triangular-lattice pattern is observed in light beams resulting from the spatial cross modulation between an optical vortex and a triangular shaped beam undergoing parametric interaction. Both up- and downconversion processes are investigated, and the far-field image of the converted beam exhibits a triangular lattice. The number of sites and the lattice orientation are determined by the topological charge of the vortex beam. In the downconversion process, the lattice orientation can also be affected by phase conjugation. The observed cross modulation works for a large variety of spatial field structures. Our results show that modulation of light by light can be used at wavelengths for which solid-state devices are not yet available. © 2022 Optica Publishing Group under the terms of the Optica Open Access Publishing Agreement

1. INTRODUCTION

The cross talk between spatial structures in nonlinear wave mixing is widely relevant in both classical and quantum regimes. The nonlinear optical process of parametric downconversion (PDC) has been extensively employed to generate quantum states of light structured in the transverse spatial degrees of freedom [1]. In the classical regime, the same process can be operated in the stimulated emission mode (StimPDC) [2,3], providing a convenient platform for the design of quantum optical schemes [4–6], and for the study of the interplay between the spatial structures of the interacting light fields in the parametric process [7–11]. In the same way, parametric upconversion plays an important role in a wide variety of applications in quantum and classical optical schemes, as, for instance, frequency conversion of squeezed light fields [12,13] and imaging with visible and invisible light [14,15]. The spatial structure of light beams, including the so-called optical vortex [16], gives rise to interesting effects in upconversion [17–21]. Therefore, frequency conversion of structured light paves the way for an increasing number of applications [22,23].

In the present work, we investigate the fields generated in the process of parametric upconversion and stimulated downconversion. It is known that the nonlinear evolution of optical vortex beams undergoing parametric up- and downconversion is subjected to selection rules, which determine orbital angular momentum (OAM) conservation as a ubiquitous condition [8,17], and the appearance of radial modes as a possible side effect depending on the relative chirality of the interacting beams [24–28]. Both conditions naturally appear from the straightforward calculation of the spatial overlap between the interacting modes. However, a more appealing physical picture is to consider the propagation properties of the outgoing field as a result of the spatial cross modulation due to the nonlinear interaction between incoming beams, which is equivalent to diffraction through an aperture.

Exploiting this simple physical picture, we demonstrate the occurrence of one striking effect in the diffraction phenomena of vortex beams generated in the nonlinear optical process, namely, the formation of a triangular lattice in far-field patterns [29–31].

We observe this outcome in both frequency up- and downconversion by mixing a vortex beam with a triangular shaped beam. The triangular lattice in the converted field evinces the effect, and the lattice orientation and number of sites are determined by the topological charge of the incoming vortex beam. In the downconversion process, the lattice orientation is also affected by phase conjugation [7,32], depending on whether the vortex structure is prepared in the pump or seed beam. Our findings advance the understanding of the role of spatial transverse structures in light fields generated from interaction in a nonlinear medium. Moreover, the fact that these fields have different wavelengths for the pump and seed allows wavefront manipulation and sensing in frequency ranges for which there are no commercial modulation devices.

2. SPATIAL CROSS MODULATION IN NONLINEAR WAVE MIXING

The wave mixing of two input signals inside a nonlinear crystal generates a new field contribution, which is coherently amplified along the interaction length, provided the phase matching condition is fulfilled. Pphase matching implies a constraint between the wave vectors of the interacting fields [33]. In the paraxial regime, it is useful to analyze this constraint separately in longitudinal and transverse directions. In the case of an optically thin nonlinear medium, the bandwidth of the longitudinal phase matching is large, and the spatial profile of the field generated in the nonlinear interaction is essentially determined by the product of the transverse structures carried by the input beams [34]. The output field carries the combined information of the input beams, in a situation that is quite equivalent to usual diffraction problems, where the field distribution immediately after an obstacle is the product between the incident field distribution and the transmission function $\mathcal{T}(\mathbf{r})$ that characterizes the obstacle: $\mathcal{E}_{\text{out}}(\mathbf{r}) = \mathcal{T}(\mathbf{r})\mathcal{E}_{\text{in}}(\mathbf{r})$. Therefore, the patterns generated in nonlinear wave mixing can be viewed as an effective diffraction problem where one input beam plays the role of an obstacle or spatial modulator. We next analyze the up- and downconversion processes separately, demonstrating the striking triangular pattern formed by transmission of an optical vortex through a triangular aperture.

Upconversion. In the upconversion configuration, two input beams $\mathbf{E}_1$ and $\mathbf{E}_2$ are mixed in the nonlinear medium and generate the output field $\mathbf{E}_3$, satisfying energy $\omega_1 + \omega_2 = \omega_3$ and momentum $\mathbf{k}_1 + \mathbf{k}_2 = \mathbf{k}_3$ conservation. Each field component carries a spatial structure $\mathcal{E}_j(\mathbf{r})$ ($j = 1, 2, 3$) and a polarization unit vector $\hat{\boldsymbol{e}}_j$, so that

$$\mathbf{E}_j = \mathcal{E}_j(\mathbf{r})\hat{\boldsymbol{e}}_j. \tag{1}$$

The spatial structure of the upconverted beam is proportional to the product of those carried by the incoming beams [26,27]:

$$\mathcal{E}_3(\mathbf{r}) = g\mathcal{E}_1(\mathbf{r})\mathcal{E}_2(\mathbf{r}), \tag{2}$$

where g is the effective coupling constant. Therefore, the pattern formed by the upconverted beam after the interaction region corresponds to the cross modulation between the input (usually infrared) beams. In this sense, the resulting pattern can be viewed as the diffraction of one beam through an effective transmission function embodied by the other. This interpretation is illustrated in Fig. 1 (left panel).

Stimulated parametric downconversion. In the stimulated downconversion configuration (StimPDC), two input beams $\mathbf{E}_p$ (pump) and $\mathbf{E}_s$ (seed) are mixed in the nonlinear medium and generate the output field $\mathbf{E}_i$ (idler), satisfying energy $\omega_p - \omega_s = \omega_i$ and momentum $\mathbf{k}_p - \mathbf{k}_s = \mathbf{k}_i$ conservation. Each field component has a spatial structure $\mathcal{E}_j(\mathbf{r})$ ($j = p, s, i$) and a polarization unit vector $\hat{\boldsymbol{e}}_j$, as before. The spatial structure of the downconverted beam is proportional to the product between the structure carried by the pump and the conjugate of the one carried by the seed beam [7]:

$$\mathcal{E}_i(\mathbf{r}) = g\mathcal{E}_p(\mathbf{r})\mathcal{E}_s^*(\mathbf{r}), \tag{3}$$

where g is the effective coupling constant. Therefore, the pattern formed by the downconverted beam after the interaction region corresponds to the cross modulation between the pump and the conjugate seed structures. In this case, the role of the effective transmission function is played differently by the pump and seed beams. Figure 1 (right panel) illustrates the situation of having the triangular aperture in the pump field.

3. EXPERIMENT

Upconversion setup. We start by describing the experiment of sum-frequency generation. The experimental setup is sketched in Fig. 2(a). The horizontally polarized Gaussian beam is produced by a 100 mW, c.w. Nd:YAG laser ($\lambda = 1064$ nm), which is split in a beam splitter (BS). One spatial light modulator (SLM) divided in two panels is used to produce a triangular-shaped beam, which

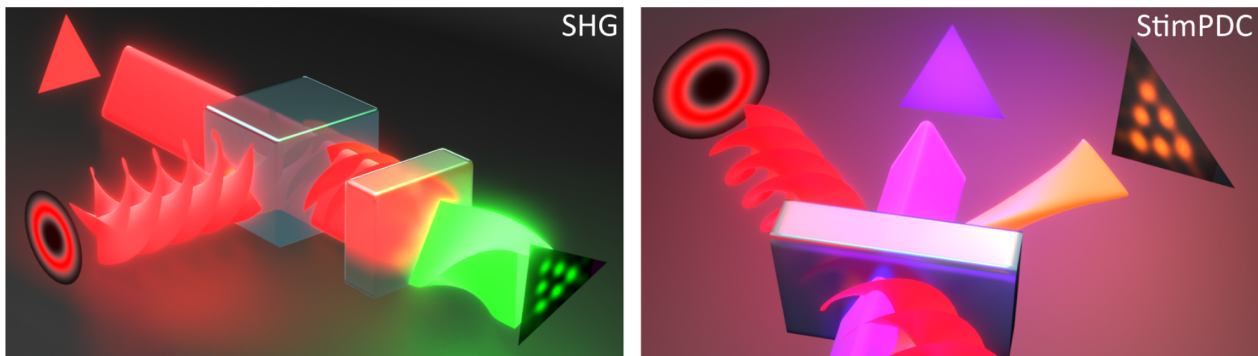**Fig. 1.** Cross modulation of light fields in nonlinear wave mixing. Left panel: input fields (in red) with orthogonal polarizations, equal frequencies, and different spatial structures incident on a polarizing beam splitter for second-harmonic generation (SHG). Right panel: input fields of different frequencies and spatial structures (in red and purple) in stimulated parametric downconversion (StimPDC).
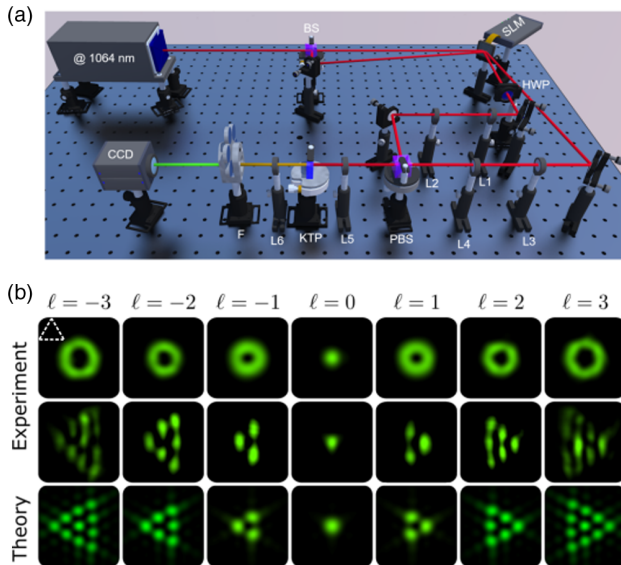
(a)

(b)

Fig. 2. (a) Experimental scheme for spatial cross modulation in upconversion. BS, beam splitter; SLM, spatial light modulator; HWP, half-wave plate; L1–L6, lenses; PBS, polarizing beam splitter; KTP, potassium titanyl phosphate nonlinear crystal; F, bandpass filter; CCD, camera. The power ratio between triangle and LG beam is one. (b) Measured far-field intensity patterns for the LG input fields (top row) and for the upconverted ones (middle row). The bottom row shows the theoretical upconverted patterns. The dashed white triangle illustrates the orientation of the triangular beam.

is transmitted, and also a Laguerre–Gaussian (LG) mode that is reflected by the BS. In both cases, we use the standard modulation approach based on blazed phase gratings and forked masks for the LG modes. To preserve the transverse structure along the propagation to the nonlinear crystal, we use $4f$ imaging lens systems ($f = 10$ cm) L1/L2 and L3/L4 in upper and lower paths, respectively. The polarization for proper phase matching is set by a half-wave plate oriented at $45°$ in the path of the triangular beam, resulting in vertical polarization. The beams are focused on a potassium titanyl phosphate (KTP) crystal cut for type-II phase matching using a 10 cm focal length lens. A bandpass filter is used to prevent the non-converted infrared beams from reaching the CCD camera, while the upconverted green light ($\lambda = 532$ nm) is imaged after collimation by a 10 cm focal length lens. Far-field intensity profiles are registered with the camera.

Figure 2(b) displays the experimental results for LG input beams having topological charges ranging from -3 to $+3$. The images in the upper row show the measured LG beam intensity profiles. In the second and bottom rows, the measured and theoretical far-field intensity patterns for the upconverted beam are respectively shown.

StimPDC setup. We have also investigated the StimPDC process. The sketch of the experimental setup is shown in Fig. 3(a). We use a vertically polarized, 30 mW, c.w. 405 nm laser beam to pump a beta barium borate (BBO) nonlinear crystal. The beam is transmitted through a *mechanical (not SLM)* triangular aperture, and then imaged in the crystal plane using a 30 cm focal length lens. As the seed beam, we use laser light of 780 nm wavelength and horizontal polarization. We use a SLM to shape the seed beam as LG modes, and the SLM plane is imaged onto the crystal plane using a 30 cm focal length lens. The pump beam is incident nearly perpendicular to the BBO crystal surface, while the seed beam
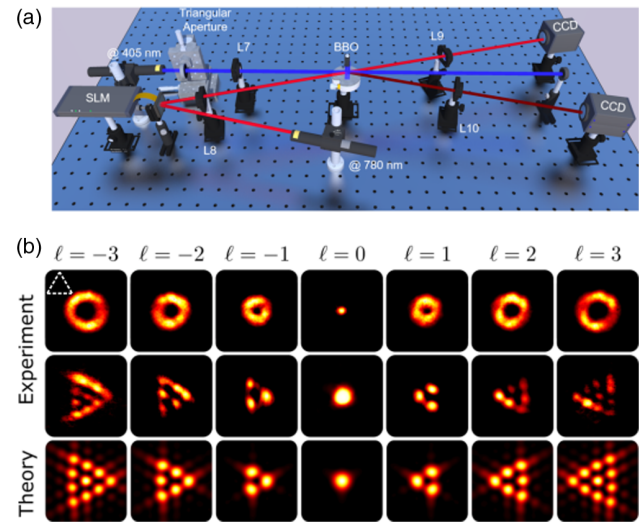
(a)

(b)

Fig. 3. (a) Experimental scheme for spatial cross modulation in stimulated downconversion. SLM, spatial light modulator; L7–L10, lenses; BBO, beta barium borate nonlinear crystal; CCD, camera. The power ratio between triangle and LG beam is two. (b) Measured far-field intensity patterns for LG seed (top row) and idler (middle row) fields. The bottom row shows the theoretical idler patterns. The dashed white triangle illustrates the orientation of the triangular beam.

is incident at about 4 deg with respect it. The far-field intensity distributions of both seed and idler beams are registered by CCD cameras with the aid of 40 cm focal length lenses.

Similar to the upconversion measurements, we used LG seed beams having topological charges ranging from -3 to $+3$. The results are shown in Fig. 3(b). The top row displays the measured LG beam intensity profiles. Images of the measured and theoretically calculated far-field intensity patterns of the idler beam are shown in the middle and bottom rows, respectively.

4. DISCUSSION

Figures 2(b) and 3(b) demonstrate the good agreement between experimental and theoretical intensity patterns. For each conversion process alone, we observe the formation of a triangular lattice with topological charge $|\ell| = N - 1$, where N is the number of high intensity lobes at the edges, and orientation is dependent on the sign of ℓ. These results reinforce the physical picture presented above, since they follow what is observed when diffracting a LG beam through a triangular aperture [29].

The opposite orientations of the triangular lattices for upconversion and StimPDC emphasize the phase conjugation effect existing only in StimPDC. Equation (3) shows the dependence of the idler field on the phase conjugated seed field $\mathcal{E}_s^*(\mathbf{r})$. In this case, because the seed is prepared as a LG beam with topological charge $+\ell$, the triangular lattice formed in the idler looks like it was the diffraction of a $-\ell$ beam.

The results also show that the effective spatial modulation in nonlinear wave mixing is of both amplitude and phase. Even though the phase modulation effect is more clearly demonstrated for StimPDC, it also works for upconversion.

5. CONCLUSION

In conclusion, we demonstrated triangular-lattice patterns generated by nonlinear wave mixing of an optical vortex with a triangular

aperture-shaped beam, which works as a spatial modulation device. The cross modulation between input optical fields in the conversion schemes is, however, more general, and could be used to overcome the lack of devices in certain frequency ranges, whereas its counterpart in the visible range is readily available. Wavefront shaping in the THz, in the extreme ultraviolet, and in the x-ray ranges, for instance, can be achieved by using a SLM to control the visible input field. In the THz range, for instance, nonlinear optical conversion from visible light is already used to generate [35] and detect [36] THz fields, and a scheme to optically control metasurfaces generating THz radiation has been recently demonstrated [37]. In addition, wavefront sensing of telecom and x-ray fields can be accomplished by conversion to the visible range. The phase information thus transferred to the visible output field can be recorded using a common CCD camera. One example of such application is the conversion of infrared images to visibile [15] using upconversion. In the upconversion experiment of our work, we use the same kind of cross modulation for a different purpose, to demonstrate detection of topological charges.

Moreover, our scheme of StimPDC allows for filtering phase information. Recently, Rocha *et al*. [38] introduced a way of filtering the random phase from speckles through nonlinear wave mixing. The configuration presented there works only if the conjugate phase is present in one of the patterns, a restriction that is naturally lifted in StimPDC. A possible application would be using a random phase or medium as an encryption key in optical communication. An image (seed beam) encodes information, which is transferred to the idler beam in StimPDC. The decoded information would be obtained by propagating the idler through the key. Directly filtering the random phase in a speckle pattern is of paramount importance also to imaging systems, and mode sorters, where the information is commonly achieved through computationally extensive post-processing using statistical correlation.

Our findings advance the knowledge of the role of spatially structured light in nonlinear wave mixing. The theoretical modeling and experimental control of frequency conversion processes is crucial in applications such as quantum communication and quantum memories and relays [39].

Disclosures. The authors declare no conflicts of interest.

Data availability. The data analyzed in the presented research are included in the main text.

REFERENCES

1. S. Walborn, C. Monken, S. Pádua, and P. Souto Ribeiro, "Spatial correlations in parametric down-conversion," Phys. Rep. **495**, 87–139 (2010).
2. Z. Y. Ou, L. J. Wang, and L. Mandel, "Photon amplification by parametric downconversion," J. Opt. Soc. Am. B **7**, 211–214 (1990).
3. Z. Y. Ou, L. J. Wang, X. Y. Zou, and L. Mandel, "Coherence in two-photon down-conversion induced by a laser," Phys. Rev. A **41**, 1597–1601 (1990).
4. M. Liscidini and J. E. Sipe, "Stimulated emission tomography," Phys. Rev. Lett. **111**, 193602 (2013).
5. L. A. Rozema, C. Wang, D. H. Mahler, A. Hayat, A. M. Steinberg, J. E. Sipe, and M. Liscidini, "Characterizing an entangled-photon source with classical detectors and measurements," Optica **2**, 430–433 (2015).
6. M. A. Ciampini, A. Geraldi, V. Cimini, C. Macchiavello, J. E. Sipe, M. Liscidini, and P. Mataloni, "Stimulated emission tomography: beyond polarization," Opt. Lett. **44**, 41–44 (2019).
7. P. H. Souto Ribeiro, D. P. Caetano, M. P. Almeida, J. A. Huguenin, B. C. dos Santos, and A. Z. Khoury, "Observation of image transfer and phase conjugation in stimulated down-conversion," Phys. Rev. Lett. **87**, 133602 (2001).
8. D. P. Caetano, M. P. Almeida, P. H. Souto Ribeiro, J. A. O. Huguenin, B. C. dos Santos, and A. Z. Khoury, "Conservation of orbital angular momentum in stimulated down-conversion," Phys. Rev. A **66**, 041801 (2002).
9. M. F. Z. Arruda, W. C. Soares, S. P. Walborn, D. S. Tasca, A. Kanaan, R. M. de Araújo, and P. H. S. Ribeiro, "Klyshko's advanced-wave picture in stimulated parametric down-conversion with a spatially structured pump beam," Phys. Rev. A **98**, 023850 (2018).
10. A. G. de Oliveira, M. F. Z. Arruda, W. C. Soares, S. P. Walborn, R. M. Gomes, R. M. de Araújo, and P. H. S. Ribeiro, "Real-time phase conjugation of vector vortex beams," ACS Photon. **7**, 249–255 (2020).
11. A. G. de Oliveira, N. R. da Silva, R. M. de Araújo, P. H. S. Ribeiro, and S. P. Walborn, "Quantum optical description of phase conjugation of vector vortex beams in stimulated parametric down-conversion," Phys. Rev. Appl. **14**, 024048 (2020).
12. C. E. Vollmer, C. Baune, A. Samblowski, T. Eberle, V. Händchen, J. Fiurásšek, and R. Schnabel, "Quantum up-conversion of squeezed vacuum states from 1550 to 532 nm," Phys. Rev. Lett. **112**, 073602 (2014).
13. H. Kerdoncuff, J. B. Christensen, and M. Lassen, "Quantum frequency conversion of vacuum squeezed light to bright tunable blue squeezed light and higher-order spatial modes," Opt. Express **29**, 29828–29840 (2021).
14. A. Barh, P. J. Rodrigo, L. Meng, C. Pedersen, and P. Tidemand-Lichtenberg, "Parametric upconversion imaging and its applications," Adv. Opt. Photon. **11**, 952–1019 (2019).
15. X. Qiu, F. Li, W. Zhang, Z. Zhu, and L. Chen, "Spiral phase contrast imaging in nonlinear optics: seeing phase objects using invisible illumination," Optica **5**, 208–212 (2018).
16. M. J. Padgett, "Orbital angular momentum 25 years on invited," Opt. Express **25**, 11265–11274 (2017).
17. K. Dholakia, N. B. Simpson, M. J. Padgett, and L. Allen, "Second-harmonic generation and the orbital angular momentum of light," Phys. Rev. A **54**, R3742–R3745 (1996).
18. D. S. Ether, P. H. S. Ribeiro, C. H. Monken, and R. L. de Matos Filho, "Effects of spatial transverse correlations in second-harmonic generation," Phys. Rev. A **73**, 053819 (2006).
19. Y. Zhang, J. Wen, S. N. Zhu, and M. Xiao, "Nonlinear Talbot effect," Phys. Rev. Lett. **104**, 183901 (2010).
20. X.-H. Hong, B. Yang, C. Zhang, Y.-Q. Qin, and Y.-Y. Zhu, "Nonlinear volume holography for wave-front engineering," Phys. Rev. Lett. **113**, 163902 (2014).
21. H. Liu, X. Zhao, H. Li, Y. Zheng, and X. Chen, "Dynamic computer-generated nonlinear optical holograms in a non-collinear second-harmonic generation process," Opt. Lett. **43**, 3236 (2018).
22. F. Steinlechner, N. Hermosa, V. Pruneri, and J. P. Torres, "Frequency conversion of structured light," Sci. Rep. **6**, 21390 (2016).
23. H.-J. Wu, B.-S. Yu, Z.-H. Zhu, W. Gao, D.-S. Ding, Z.-Y. Zhou, X.-P. Hu, C. Rosales-Guzmán, Y. Shen, and B.-S. Shi, "Conformal frequency conversion for arbitrary vectorial structured light," Optica **9**, 187–196 (2022).
24. W. T. Buono, L. F. C. Moraes, J. A. O. Huguenin, C. E. R. Souza, and A. Z. Khoury, "Arbitrary orbital angular momentum addition in second harmonic generation," New J. Phys. **16**, 093041 (2014).
25. L. J. Pereira, W. T. Buono, D. S. Tasca, K. Dechoum, and A. Z. Khoury, "Orbital-angular-momentum mixing in type-ii second-harmonic generation," Phys. Rev. A **96**, 053856 (2017).
26. W. T. Buono, J. Santiago, L. J. Pereira, D. S. Tasca, K. Dechoum, and A. Z. Khoury, "Polarization-controlled orbital angular momentum switching in nonlinear wave mixing," Opt. Lett. **43**, 1439–1442 (2018).
27. W. T. Buono, A. Santos, M. R. Maia, L. J. Pereira, D. S. Tasca, K. Dechoum, T. Ruchon, and A. Z. Khoury, "Chiral relations and radial-angular coupling in nonlinear interactions of optical vortices," Phys. Rev. A **101**, 043821 (2020).
28. A. de Oliveira, G. Santos, N. R. da Silva, L. Pereira, G. Alves, A. Khoury, and P. H. S. Ribeiro, "Beyond conservation of orbital angular momentum in stimulated parametric down-conversion," Phys. Rev. Appl. **16**, 044019 (2021).

29. J. M. Hickmann, E. J. S. Fonseca, W. C. Soares, and S. Chávez-Cerda, "Unveiling a truncated optical lattice associated with a triangular aperture using light's orbital angular momentum," Phys. Rev. Lett. **105**, 053904 (2010).

30. L. A. Melo, A. J. Jesus-Silva, S. Chávez-Cerda, P. H. S. Ribeiro, and W. C. Soares, "Direct measurement of the topological charge in elliptical beams using diffraction by a triangular aperture," Sci. Rep. **8**, 6370 (2018).

31. Y. Shen, X. Fu, and M. Gong, "Truncated triangular diffraction lattices and orbital-angular-momentum detection of vortex SU(2) geometric modes," Opt. Express **26**, 25545–25557 (2018).

32. A. G. de Oliveira, M. F. Z. Arruda, W. C. Soares, S. P. Walborn, A. Z. Khoury, A. Kanaan, P. H. S. Ribeiro, and R. M. de Araújo, "Phase conjugation and mode conversion in stimulated parametric down-conversion with orbital angular momentum: a geometrical interpretation," Braz. J. Phys. **49**, 10–16 (2019).

33. W. Zhang, H. Yu, H. Wu, and P. S. Halasyamani, "Phase-matching in nonlinear optical compounds: a materials perspective," Chem. Mater. **29**, 2655–2668 (2017).

34. N. Bloembergen, *Nonlinear Optics* (Addison-Wesley, 1977).

35. P. Bai, Y. Zhang, T. Wang, Z. Fu, D. Shao, Z. Li, W. Wan, H. Li, J. Cao, X. Guo, and W. Shen, "Broadband THz to NIR up-converter for photon-type THz imaging," Nat. Commun. **10**, 3513 (2019).

36. B. Haase, M. Kutas, F. Riexinger, P. Bickert, A. Keil, D. Molter, M. Bortz, and G. von Freymann, "Spontaneous parametric down-conversion of photons at 660 nm to the terahertz and sub-terahertz frequency range," Opt. Express **27**, 7458–7468 (2019).

37. K. Jana, E. Okocha, S. H. Møller, Y. Mi, S. Sederberg, and P. B. Corkum, "Reconfigurable terahertz metasurfaces coherently controlled by wavelength-scale-structured light," Nanophotonics **11**, 787–795 (2021).

38. J. C. A. Rocha, D. G. Pires, J. G. M. N. Neto, A. J. Jesus-Silva, N. M. Litchinitser, and E. J. S. Fonseca, "Speckle filtering through nonlinear wave mixing," Opt. Lett. **46**, 3905–3908 (2021).

39. D. Castelvecchi, "Quantum network is step towards ultrasecure internet," Nature **590**, 540–541 (2021).